International Journal of the Physical Sciences Vol. 6(25), pp. 6036-6041, 23 October, 2011
Available online at http://www.academicjournals.org/IJPS
DOI: 10.5897/IJPS10.618
ISSN 1992 - 1950 ©2011 Academic Journals

Full Length Research Paper

Variability of El Niño-Southern oscillation from 1880 to 2010 revealed by wavelet analysis

Mahdi Haddad[1]*, Mohamed Faouzi Belbachir[2] and Salem Kahlouche[1]

[1]Centre of Space Techniques, Division of Space Geodesy, 1 Avenue de Palestine, BP 13 Arzew, Oran 31200, Algeria.
[2]Faculty of Electrical and Electronics Engineering,University of Sciences and Technology, Oran-Mohamed Boudiaf, BP 1505, EL M'Naouer, Oran 31000, Algeria.

Accepted 23 August, 2011

The El Niño-Southern oscillation (ENSO) is shown to have undergone significant changes in variance and coherency over the last 130 years. Wavelet analysis is applied to sea surface temperature anomalies (Niño3 SSTA) index to obtain frequencies of the temporal variations in the signal. This technique works in terms of specific events while allowing a researcher to keep an eye on the ensemble properties. By using this relatively new method, our study aims at investigating a quantitative measure of changes in ENSO variance on long-term time scales. Using ERSST.v3b SSTA averaged over the Niño3 region (5 N-5 S 150-90 W) that extend back to 1880, the wavelet analysis show significantly higher events during 1885 to 1920 and 1960 to 2005, and lower events during 1920 to 1960. Most of the power is concentrated within the ENSO band of 2 to 8 years.

Key words: Morlet wavelet, Niño3 region, sea surface temperature anomalies, variability, wavelet power spectra.

INTRODUCTION

In the literature, El Niño/La Niña-Southern oscillation, or ENSO, is a climate pattern that occurs across the tropical Pacific ocean on average every five years, but over a period which varies from three to seven years, and is therefore, widely and significantly, known as "quasi-periodic". ENSO is composed of two components: an ocean temperature component, called El Niño (or La Niña, in the cooling phase), which is characterized by warming or cooling of surface waters in the tropical eastern Pacific ocean, and an ocean atmosphere component, the Southern oscillation, which is characterized by changes in air surface pressure in the tropical western Pacific. The two components are coupled: when the warm oceanic phase (known as El Niño) accompanies high air surface pressure (known as Southern oscillation) in the west Pacific, or when the cold phase (La Niña) accompanies low air surface pressure (also Southern oscillation) in the west Pacific (Trenberth et al., 2007). In popular usage, El Niño-Southern oscillation is often called just "El Niño". "El Niño is Spanish for "the boy" and refers to the Christ child, because periodic warming in the Pacific near South America is usually noticed around Christmas".

Monitoring of ENSO conditions primarily focuses on sea surface temperature anomaliesSSTA (variations from an average or other statistical reference value) in the equatorial Pacific. SSTA is equal to or greater than 0.5°C in the Niño3 region (5 N-5 S 150-90 W), or when SSTA in the Niño3.4 region (5 N-5 S 170-120 W) exceed 0.4°C, are indicative of ENSO warm phase (El Niño) conditions (Trenberth, 1997). While anomalies less than or equal to -0.5°C (or -0.4°C for the Niño3.4 region) are associated with cool phase (La Niña) conditions.

According to the NOAA/Climate Prediction Center (2005-12-19), El Niño and La Niña episodes typically occur every 3 to 5 years. However, in the historical record this interval has varied from 2 to 7 years. El Niño typically lasts 9 to 12 months, and La Niña typically lasts 1 to 3 years. They both tend to develop during March to June, reach peak intensity during December to April, and then weaken during May to July. However, prolonged El Niño episodes have lasted 2 years and even as long as 3 to 4 years. It has also been suggested that the interannual variability associated with ENSO is high during 1880 to 1920 and 1960 to 1990 and low during 1920 to 1960 (Torrence and Compo, 1998; Kestin et al., 1998; Mestas-Nuñez and Enfield, 2001).

The purpose of this paper is to give a detailed description

*Corresponding author. E-mail: haddad_mahdi@yahoo.fr.

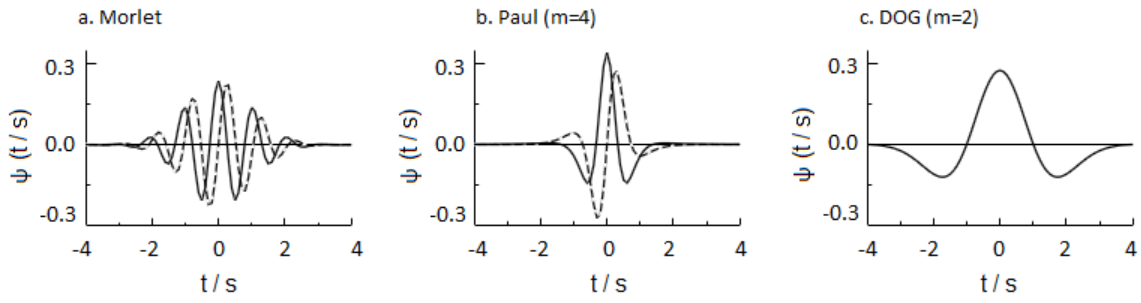

Figure 1. Mother wavelets: (a) Morlet, real and imaginary parts in solid and dashed lines, respectively; (b) Paul, with m= 4; (c) Derivative of a Gaussian (DOG), with m=2.

description of the changes in interannual variability of the ENSO during the last 130 years, through the recent ERSST.v3b SSTA (National Climatic Data Center - NCDC), by using the wavelet analysis technique. The El Niño/ La Niña events are monitored here by the Niño3 SSTA index, consisting of the area-average SSTA over the Niño3 region, monthly from 1880 to present.

Wavelets analysis functions are becoming common mathematical tools that cut up data into different frequency components, and then studying of each component with a resolution matched to its scale. They have advantages over traditional Fourier methods in analyzing physical situations where the signal contains discontinuities and sharp spikes. Several applied fields are making use of wavelets such as astronomy, acoustics, data compression, nuclear engineering, sub-band coding, signal and image processing, neurophysiology, music, magnetic resonance imaging, speech discrimination, optics, fractals, radar, human vision, pure mathematics applications such as solving partial differential equations and geophysics applications such as tropical convection (Weng and Lau, 1994), the El Niño-Southern oscillation (Gu and Philander, 1995; Wang and Wang, 1996), atmospheric cold fronts (Gamage and Blumen, 1993), central England temperature (Baliunas et al., 1997), the dispersion of ocean waves (Meyers et al., 1993), wave growth and breaking (Liu, 1994), coherent structures in turbulent flows (Farge, 1992) and stream flow characterization (Santos et al., 2001).

WAVELET TRANSFORM

The wavelet analysis in this paper follows the methods of Torrence and Compo (1998), although, the basic components and methods of wavelet analysis are reviewed here, readers are referred to Torrence and Compo (1998) for a more detailed explanation of the analysis.

There are several mathematical transformations that can be applied, among which the Fourier transforms are probably by far the most popular. However, the wavelet transform can be used to analyze time series that contain non-stationary power at many different frequencies (Torrence and Compo, 1998), because the wavelet analysis maintains time and frequency localization in a signal analysis by decomposing or transforming a one-dimensional time series into a diffuse two-dimensional time-frequency image, simultaneously. Then, it is possible to get information on both the amplitude of any “periodic” signals within the series, and how this amplitude varies with time. Examples of basic waves or mother wavelets, as they are known in the literature and are given in this study (Torrence and Compo, 1998) are shown in Figure 1. These mother wavelets have the advantage of incorporating a wave of a certain period, as well as being finite in extent.

The wavelet analysis always uses a wavelet of the exact same shape, only the size scales is up or down with the size of the window. In addition to the amplitude of any periodic signals, it is worth getting information on the phase. The Morlet wavelet was chosen for this analysis, because it has relatively good resolution in frequency when compared with other wavelets, such as the Paul wavelet, which has better resolution in time. Furthermore, it has also been used previously in both hydrological and meteorological applications (Torrence and Compo, 1998; Labat et al., 2000; Lafrenière and Sharp, 2003). In practice, the Morlet wavelet shown in Figure 1a is defined as the product of a complex exponential wave and a Gaussian envelope:

$$\psi_0(\eta) = \pi^{-1/4} e^{i\omega_0\eta} e^{-\eta^2/2} \qquad (1)$$

where $\psi_0(\eta)$ is the wavelet value at nondimensional time η and $\omega_0$is the nondimensional frequency equal to 6 in this study in order to satisfy an admissibility condition, that is, the function must have zero mean and be localized in both time and frequency space to be “admissible” as a wavelet (Farge, 1992). This is the basic wavelet function, but it will be now needed some way to change the overall size as well as slide the entire wavelet along in time. Thus, the “scaled wavelets” are defined as:

$$\Psi\left[\frac{(n'-n)\delta t}{s}\right] = \left(\frac{\delta t}{s}\right)^{1/2} \Psi_0\left[\frac{(n'-n)\delta t}{s}\right] \qquad (2)$$

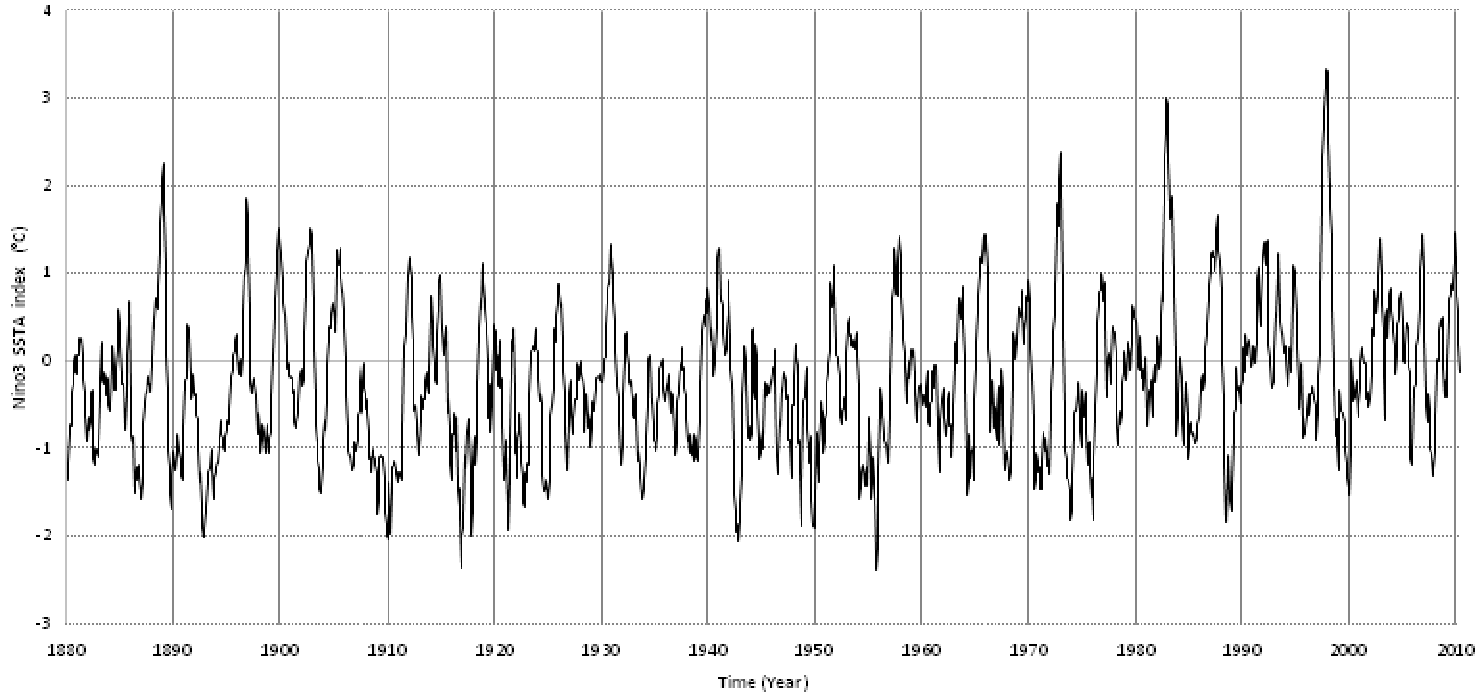

Figure 2. The Niño3 SSTA (ERSST.v3b) time series used for the wavelet analysis. Data normalized to 1971 to 2000.

where s is the "dilation" parameter used to change the scale and n is the translation parameter used to slide in time. The factor of $s^{-1/2}$ is a normalization to keep the total energy of the scaled wavelet constant. We are given a time series X, with values of x_n, at time index n. Each value is separated in time by a constant time interval δt. The wavelet transform $W_n(s)$ is just the inner product (or convolution) of the wavelet function with the original time series:

$$W_n(s) = \sum_{n'=0}^{N-1} x_{n'} \psi^* \left[\frac{(n'-n)\delta t}{s}\right] \quad (3)$$

where the asterisk (*) indicates the complex conjugate.

By sliding this wavelet along the time series, a new time series of the projection amplitude versus time can be constructed. Finally, the "scale" of the wavelet can be varied by changing its width.

DATA USED

The SSTA data sets used here was obtained from the most recent version (v3b) of the NCDC extended reconstruction sea surface temperatures (ERSST) analysis, monthly from January 1880 to June 2010. ERSST.v3b wasgenerated using in situ SST (sea surface temperature) data and improved statistical methods that allow stable reconstruction using sparse data. The monthly analysis extends from January 1854 to the present, but because of sparse data in the early years, the analyzed signal was damped before 1880. After 1880, the strength of the signal was more consistent over time. ERSST is suitable for long-term global and basin wide studies; local and short-term variations have been smoothed in ERSST. The ERSST.v3b analysis is exactly as described in the ERSST.v3 paper (Smith et al., 2008) with one exception: satellite SST data are not used in ERSST.v3b.

The used Niño3 index was computed as an average of SSTA over the eastern tropical Pacific (approximately 5°S to 5°N, 90°W to 150°W), with respect to a 1971 to 2000 month climatology (Xue et al., 2003). Figure 2 represents the used averaged SSTA time series (1880 to present) over the Niño3 region. Figure 2 shows the recent strongest El Niño / La Niña episodes. The two recent severe El Niño episodes occurred in 1982 to 1983 and in 1997 to 1998. The El Niño 1982 to 1983 began in May 1982 (unusually late). The average SSTA reached a value of 3°C in December 1982. The El Niño of 1997 to 1998 was extremely severe. This event was a so-called "Type 1" El Niño, having the strongest averaged SSTA >3.0°C during October 1997 to January 1998. Although it started in April to May 1997, its effects extended into early summer 1998.

There was a strong recent La Niña episode occurring in 1988 to 1989, having the strongest averaged SSTA <-1.25°C during May 1988 to January 1989. Severe La Niña was also formed in 1998 to 2000. From June 2007, data indicated a moderate La Niña event, which strengthened until early 2008. The 2007 to 2008 La Niña event was the strongest since the 1988 to 1989 event.

Figure 3 illustrates the remarkable opposite phases of the 1997 to 1998 ENSO cycle. Normal Equatorial Pacific ocean surface temperatures and winds velocities (December 1993) are shown in Figure 3b, including cool water in the Eastern Pacific and warm water in the Western Pacific. Strong La Niña conditions during December 1998 are shown in Figure 3a. The Eastern Pacific is cooler than usual, and the cool water extends farther westward than is usual. Strong El Niño conditions, in December 1997, are shown in Figure 3c, with warm water extending all along the equator.

DATA ANALYSIS

In order to study the variability of ENSO, the wavelet

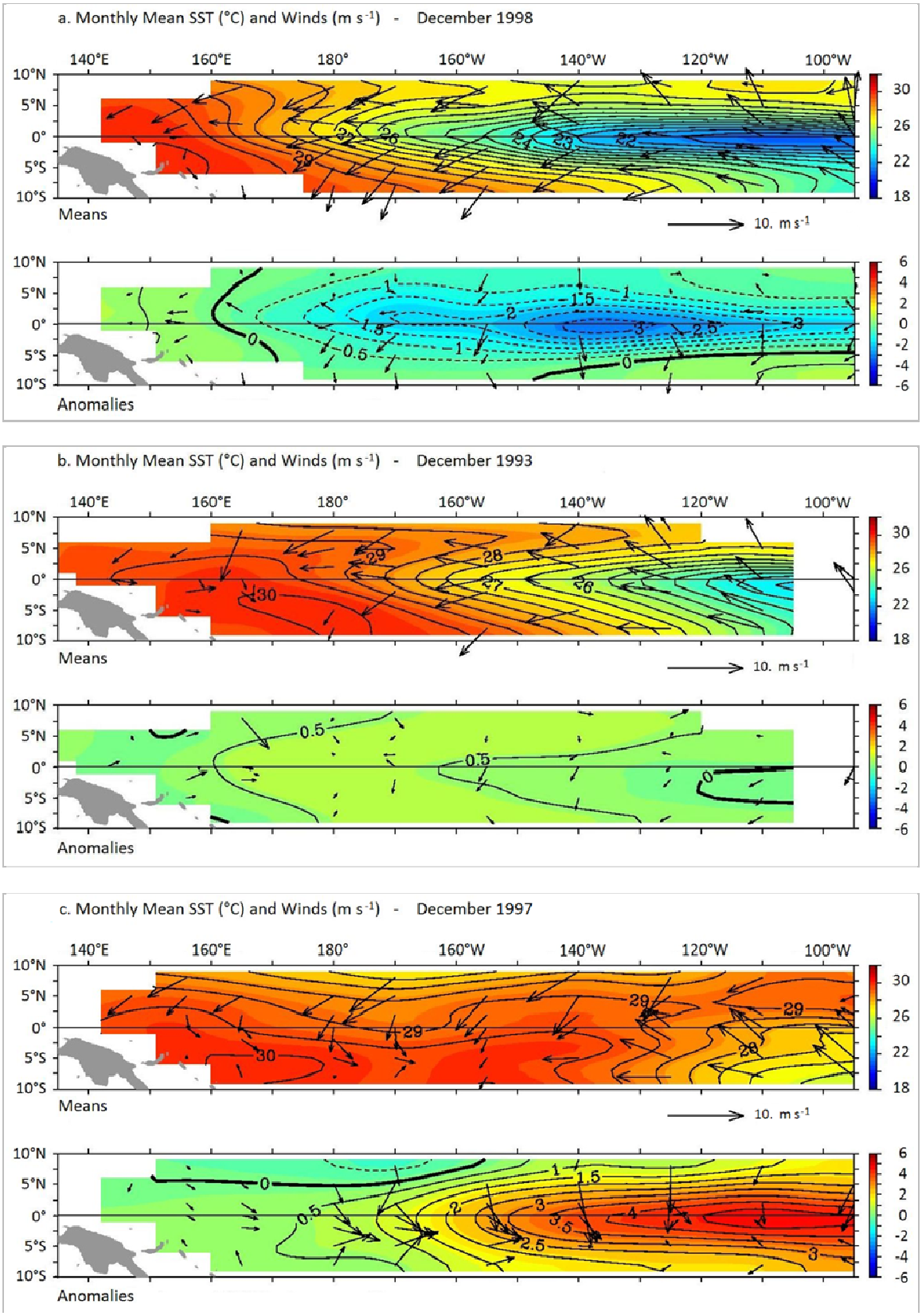

Figure 3. Remarkable opposite phases of the 1997 to 1998 ENSO cycle: (a) La Niña (December 1998), a colder than normal event; (b) Normal conditions (December 1993); (c) El Niño (December 1997) a warmer than normal event. Graphics are provided by the Tropical Atmosphere Ocean (TAO) project office/NOAA.

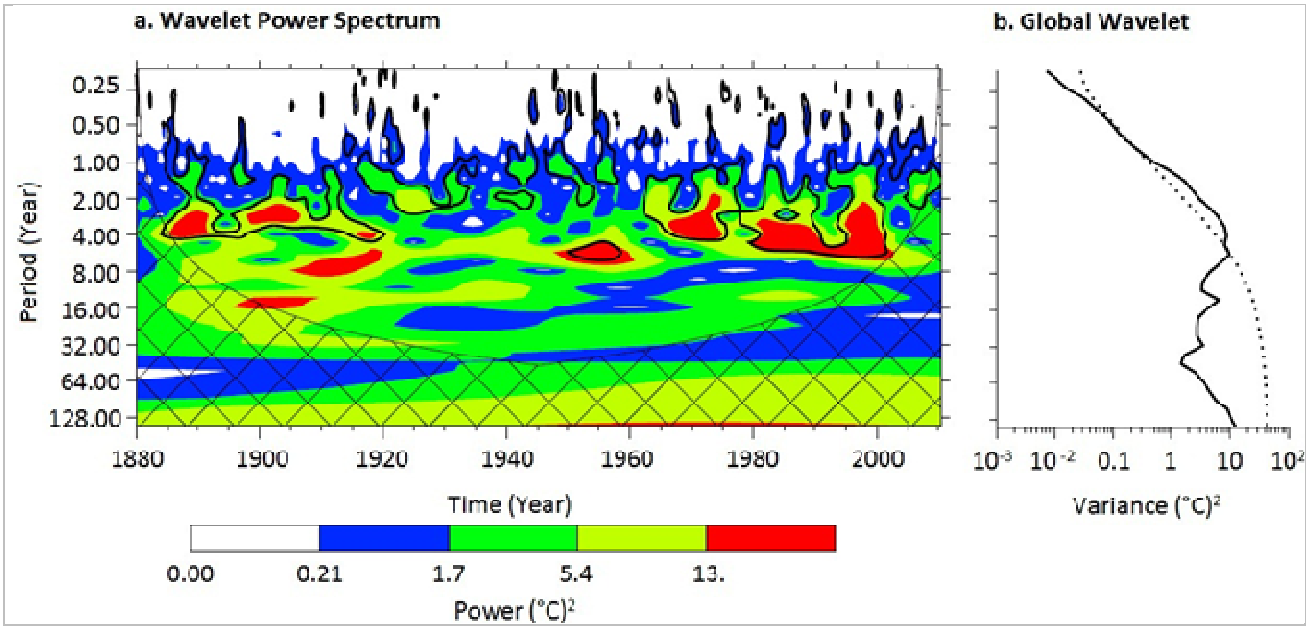

Figure 4. (a) The wavelet power spectrum, using the Morlet wavelet. The contour levels are chosen so that 75, 50, 25 and 5% of the wavelet power is above each level, respectively. The cross-hatched regions on either end indicate the "cone of influence," where edge effects become important. Black contour is the 10% significance level, using a red-noise (lag-1 autoregressive process) background spectrum. (b) The global wavelet power spectrum (black line). The dashed line is the significance for the global wavelet spectrum, assuming the same significance level and background spectrum as in (a).

power spectrum is evaluated here for the Niño3 SSTA time series. The wavelet power spectrum, which is defined as the squared modulus of the wavelet transform, provides a good description on the relative power at different scales or frequencies. Additional information about the behavior of the SSTA time series is obtained by calculating the scale-averaged wavelet power. Note that all the results and figures presented in this part are obtained by means of the wavelet analysis matlab program, provided by Torrence and Compo and is available at (http://atoc.colorado.edu/research/wavelets/).

Wavelet power spectrum analysis

Since ERSST.v3b SSTA data are monthly distributed, the parameters for the wavelet analysis are set as $\delta t = 1\ \mathrm{month}$, the smallest resolvable wavelet scale s_0 as $2\delta t$ (this says, start at a scale of 2 months). The fractional spacing between wavelet scales was chosen as 0.25, this value of δj appears adequate to provide a smooth picture of wavelet power. Given that for the continuous wavelet transform there will be problems near the edge of the time series, we pad with zeroes the end of the time series before applying the wavelet transform and then remove them afterward. This reduces the wavelet power near the edges, but it avoids wrap-around effects (Torrence and Compo, 1998). Figure 4 shows the variability constructed by plotting the power of the wavelet transform for the monthly Niño3 SSTA (1880 to present).

In Figure 4, the red areas indicate the high ENSO activity. One can see evidence that during 1885 to1920 and 1960 to 2005 there were many warm and cold events of large amplitude, while during 1920 to 1960, it was relatively calm. The wavelet power spectrum indicates also that the ENSO episodes typically occurred every 2 to 8 years. In addition, we can see hints of a 16 years oscillation (1895 to 1910).

Scale-average time series

To examine fluctuations in power over a range of scales, one can considerate the scale-averaged wavelet power. Figure 5 is made by the average of Figure 4a over all scales between 2 and 8 years (where most of ENSO events occurred) and gives a measure of the average ENSO variance versus time.

The 2 to 8 years variance plot shows distinct periods when ENSO variance was low from 1920 to 1960. An important peak in the scale-average time series can be identified for 1997 to 1998, clearly indicating the strongest warm ENSO recorded in history (see the situation of the strong December 1997 El Niño event in Figure 3c).

CONCLUSION

Wavelet analysis is a useful tool for analyzing time series with many different timescales or changes in variance. In order to study the variability of sea surface temperature

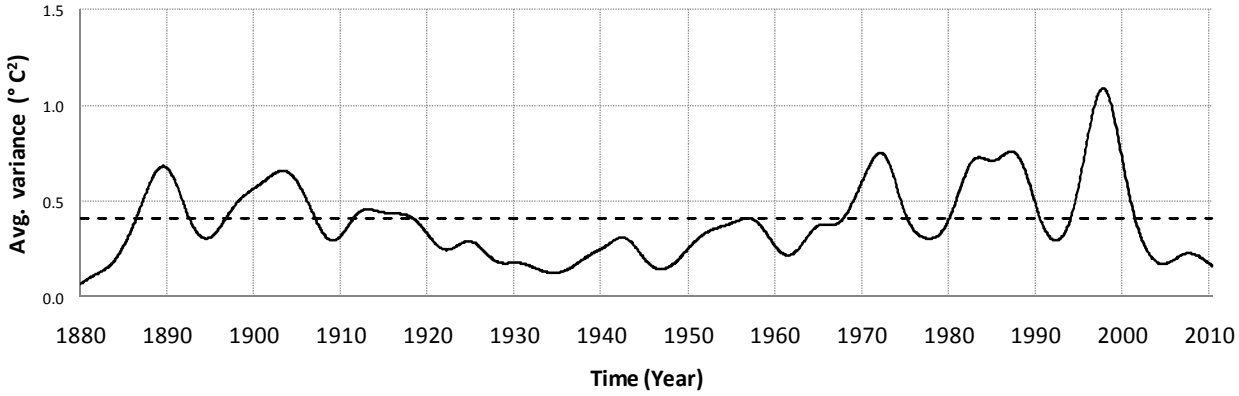

Figure 5. Scale-averaged wavelet power over the 2 to 8 years bands. The thin dashed line is the 95% confidence level.

anomaly time series (1880 to present) over the Niño3 region, wavelet analysis was applied. This analysis indicates that the intervals of high activity of the El Niño-Southern oscillation occurred from 1885 to 1920 and from 1960 to 2005. The time interval from 1920 to 1960 was relatively calm. These results agree with other studies which suggested that the interannual variability of ENSO is high during 1880 to 1920 and 1960 to 1990 and low during 1920 to 1960 (Torrence and Compo, 1998; Kestin et al., 1998; Mestas-Nuñez and Enfield, 2001).

It was also found that the most of the power is concentrated within the band of 2 to 8 years. The 2 to 8 years band for ENSO agrees with other studies (Trenberth, 1976; Torrence and Compo, 1998). Also, there is an appreciable power at longer periods of 16 years.

ACKNOWLEDGEMENTS

The authors are grateful to Dr. Christopher Torrence of ITT Visual Information Solutions and to Dr. Gilbert P. Compo of NOAA/CIRES Climate Diagnostics Center for providing the wavelet analysis computer program. The authors are also grateful to National Climatic Data Center (NCDC) for providing the ERSST.v3b SSTA data, and they greatly appreciate the anonymous reviewers for their valuable and constructive comments.

REFERENCES

Baliunas S, Frick P, Sokoloff D, Soon W (1997). Time scales and trends in the central England temperature data (1659-1990): A wavelet analysis. Geophys. Res. Lett., 24: 1351-1354.

Farge M (1992). Wavelet transforms and their applications to turbulence. Ann. Rev. Fluid. Mech., 24: 395-457.

Gamage N, Blumen W (1993). Comparative analysis of lowlevel cold fronts: Wavelet, Fourier, and empirical orthogonal function decompositions. Mon. Wea. Rev., 121: 2867-2878.

Gu D, Philander SGH (1995). Secular changes of annual and interannual variability in the Tropics during the past century. J. Climate, 8: 864-876.

Kestin TS, Karoly DJ, Yano JI, Rayner NA (1998). Time-frequency variability of ENSO and stochastic simulations. J. Climate, 11: 2258-2272.

Labat D, Ababou R, Mangin A (2000). Rainfall-runoff relations for karstic springs. Part II: continuous wavelet and discrete orthogonal multiresolution analyses. J. Hydrol., 238: 149–178.

Lafrenière M, Sharp M (2003). Wavelet analysis of inter-annual variability in the runoff regimes of glacial and nival stream catchments, Bow Lake, Alberta. Hydrol. Proc., 17: 1093-1118.

Liu PC (1994). Wavelet spectrum analysis and ocean wind waves. Wavelets in Geophysics, E. Foufoula-Georgiou and P. Kumar, Eds., Academic Press. pp. 151-166.

Mestas-Nuñez AM, Enfield DB (2001). Eastern equatorial Pacific SST variability: ENSO and non-ENSO components and their climatic associations. J. Climate, 14: 391-402.

Meyers SD, Kelly BG, O'Brien JJ (1993). An introduction to wavelet analysis in oceanography and meteorology: With application to the dispersion of Yanai waves. Mon. Wea. Rev., 121: 2858-2866.

NOAA/ Climate Prediction Center (2005-12-19). ENSO FAQ: How often do El Niño and La Niña typically occur? National Centers for Environmental Prediction. http://www.cpc.noaa.gov/products/analysis_monitoring/ensostuff/ensofaq.shtml#HOWOFTEN.

Santos CAG, Galvão CO, Suzuki K, Trigo RM (2001). Matsuyama city rainfall data analysis using wavelet transform, Ann. J. Hydraul. Engng, JSCE, 45: 211-216.

Smith TM, Reynolds RW, Peterson TC, Lawrimore J (2008). Improvements to NOAA's Historical Merged Land-Ocean Surface Temperature Analysis (1880-2006). J. Climate, 21: 2283-2296.

Torrence C, Compo GP (1998). A practical guide to wavelet analysis. Bull. Amer. Met. Soc., 79(1): 62-78.

Trenberth KE (1976). Spatial and temporal variations of the Southern Oscillation. Quart. J. Roy. Meteor. Soc., 102: 639-653.

Trenberth KE (1997). The definition of El Niño. Bull. Amer. Met. Soc., 78: 2771-2777.

Trenberth KE, Jones PD, Ambenje P, Bojariu R, Easterling D, Klein Tank A, Parker D, Rahimzadeh F, Renwick JA, Rusticucci M, Soden B, Zhai P (2007). Observations: Surface and Atmospheric Climate Change. in Solomon S, Qin D, Manning M, Chen Z, Marquis M, Averyt KB, Tignor M, Miller HL. Climate Change 2007: The Physical Science Basis. Contribution of Working Group I to the Fourth Assessment Report of the Intergovernmental Panel on Climate Change. Cambridge,UK: Cambridge University Press. pp. 235-336.

Wang B, Wang Y (1996). Temporal structure of the Southern Oscillation as revealed by waveform and wavelet analysis. J. Climate, 9: 1586-1598.

Weng H, Lau KM (1994). Wavelets, period doubling, and time-frequency localization with application to organization of convection over the tropical western Pacific. J. Atmos. Sci., 51: 2523-2541.

Xue Y, Smith TM, Reynolds RW (2003). Interdecadal changes of 30-yr SST normals during 1871-2000. J. Climate, 16: 1601-1612.